



## Proteomics-based investigation of the protective effect and mechanism of Agari-5 in rats with myocardial infarction

Journal:	<i>Science Progress</i>
Manuscript ID	SCI-25-1563
Manuscript Type:	Original Research Article
Date Submitted by the Author:	09-Jul-2025
Complete List of Authors:	Wan, Quan; Affiliated Hospital of Inner Mongolia Minzu University Zhao, Yubao; Horqin Right Wing Central Banner Mongolian Medicine Hospital Bao, Zhihong; Horqin Right Wing Central Banner Mongolian Medicine Hospital Tu, Ya; Horqin Right Wing Central Banner Mongolian Medicine Hospital Qiu, Xia; Horqin Right Wing Central Banner Mongolian Medicine Hospital Bao, Yinlan; Horqin Right Wing Central Banner Mongolian Medicine Hospital Su, Min; Horqin Right Wing Central Banner Mongolian Medicine Hospital Qi, Haijun; Horqin Right Wing Central Banner Mongolian Medicine Hospital
Keywords:	Myocardial Infarction, Agari-5, Proteomics, Protective Effect, Mechanism
Abstract:	<p>Background: Myocardial infarction occupies a very high mortality and morbidity rate, and the search for effective pharmacological treatments has far-reaching implications for clinical research.</p> <p>Methods: Sprague-Dawley rats were used, and both the Agari-5 and model groups had their coronary arteries clamped to induce myocardial infarction. Proteomics was used to research the potential mechanism of action, while ELISA, HE, and Masson were used to preliminary investigate the protective impact of Agari-5 on rats with myocardial infarction.</p> <p>Results: The current study shown that Agari-5 might enhance cardiac function indicators, including CK, CK-MB and LDH, in rats that had myocardial infarction. According to the results of pathological staining, Agari-5 may lessen inflammatory cell infiltration and cardiomyocyte fibrosis, among other things. The proteome analysis revealed that there were 60 distinct proteins in total, four of which were associated with the heart. The expression of PSAT1, PDK1, SMAD4, and SDF2 proteins may be linked to the mechanism of their protective effects.</p> <p>Conclusion: Potential therapeutic effects of Agari-5 for myocardial infarction and also, its mechanism of action may be related to PSAT1, PDK1, SMAD4 and SDF2.</p>

Proteomics-based investigation of the protective effect and mechanism of Agari-5 in rats with myocardial infarction

Yubao Zhao<sup>1</sup>, Zhihong Bao<sup>1</sup>, Ya Tu<sup>1</sup>, Xia Qiu<sup>1</sup>, Yinlan Bao<sup>1</sup>, Min Su<sup>1</sup>, Haijun Qi<sup>1</sup>, Quan Wan<sup>2\*</sup>

1. Horqin Right Wing Central Banner Mongolian Medicine Hospital, Xinganmeng, Inner Mongolia, China;

2. Affiliated Hospital of Inner Mongolia Minzu University, Tongliao, Inner Mongolia, China

Correspondence: Quan Wan, wanquan120@126.com.

Abstract:

Background: Myocardial infarction occupies a very high mortality and morbidity rate, and the search for effective pharmacological treatments has far-reaching implications for clinical research.

Methods: Sprague-Dawley rats were used, and both the Agari-5 and model groups had their coronary arteries clamped to induce myocardial infarction. Proteomics was used to research the potential mechanism of action, while ELISA, HE, and Masson were used to preliminary investigate the protective impact of Agari-5 on rats with myocardial infarction.

Results: The current study shown that Agari-5 might enhance cardiac function indicators, including CK, CK-MB and LDH, in rats that had myocardial infarction. According to the results of pathological staining, Agari-5 may lessen inflammatory cell infiltration and cardiomyocyte fibrosis, among other things. The proteome analysis revealed that there were 60 distinct proteins in total, four of which were associated with the heart. The expression of PSAT1, PDK1, SMAD4, and SDF2 proteins may be linked to the mechanism of their protective effects.

Conclusion: Potential therapeutic effects of Agari-5 for myocardial infarction and also, its mechanism of action may be related to PSAT1, PDK1, SMAD4 and SDF2.

**Key words:** Myocardial Infarction; Agari-5; Proteomics; Protective Effect; Mechanism

## 1.Introduction

Myocardial infarction (MI) is a leading cause of death globally, particularly among middle-aged and elderly populations, and is one of the four major non-communicable diseases with high mortality and morbidity rates worldwide, along with cardiovascular disease, cancer, diabetes mellitus, and chronic respiratory disease [1,2]. Myocardial infarction (MI) occurs when atherosclerotic lesions in the coronary arteries cause narrowing or occlusion, leading to hypoxia and ischemia, which result in the necrosis of myocardial tissue[3,4]. During the hypoxia-reoxygenation process of cardiomyocytes, a series of damaging changes occur in myocardial ultrastructure, energy metabolism, cardiac function, and electrophysiology, which continue to affect cardiac function and structural remodeling - key pathological processes in MI [5]. Current treatments for MI include percutaneous coronary intervention and pharmacological therapies [6], and there is growing recognition of the potential of ethnomedicine in treating this condition.

Mongolian medicine Agari-5 is a widely used traditional remedy for cardiovascular diseases, consisting of five herbs: descending incense, sumac, umeboshi, borax, and danshen. It primarily works by promoting blood circulation and resolving blood stasis, and is used to treat conditions such as vascular fever, heart deficiency heat, heart stabbing pain, hypertension, and arteriosclerosis. It is particularly effective for treating heart diseases like haye disease. The compound formula reflects the holistic approach and evidence-based principles of Mongolian medicine, offering a multi-component and multi-target therapeutic effect.

Proteomics is the study of the entire set of proteins expressed in a cell or organism, utilizing techniques such as protein purification and mass spectrometry analysis to identify and quantify proteins [7,8]. Unlike genomics, proteomics is more complex, as it seeks to understand not only the total protein expression but also various aspects like protein modifications, structures, and protein-protein interactions. This comprehensive analysis makes proteomics a critical tool for understanding disease processes and cellular metabolism.

In this study, a rat MI model was constructed, and proteomics technology was applied

to investigate the therapeutic effects of the Mongolian medicine Agari-5. By analyzing protein expression differences and utilizing bioinformatics methods, the study aimed to elucidate the molecular basis and advantages of Agari-5 in treating MI [9]. The research focused on uncovering the protein-level mechanisms behind Agari-5's multi-target, multi-pathway, and multifunctional therapeutic effects, providing insights into the compound's mechanism of action. These findings will offer a theoretical basis for the use of Agari-5 in treating cardiovascular diseases and guiding future research.

**2. Materials and methods**

**2.1 Drugs and experimental reagents**

Agari-5 (No. M20201334000) was obtained from DL-Dithiothreitol (Solarbio), Iodoacetamide (Aladdin), and Tetraethylammonium bromide (Sigma). Creatine kinase (CK), creatine kinase isoenzyme (CK-MB), lactate dehydrogenase (LDH), and amino-terminal brain natriuretic peptide precursor (NT-Pro BNP) were supplied by Enzyme Free Biotechnology Ltd. Other reagents, such as ethylene diamine tetraacetic acid (EDTA), xylene brilliant cyanine G, and sodium dodecyl sulfate (SDS), were sourced from Sinopharm Chemical Reagent Co..

**2.2 Laboratory animals and ethics**

Animal experiments were conducted in compliance with the guidelines set by the Experimental Animal Ethics Committee of the Affiliated Hospital of Inner Mongolia University for Nationalities (Approval No.NM-LL-2024-05-16-08). The study followed the National Institute of Health Guidelines for the Ethical Use of Animals. Sprague-Dawley (SD) rats were obtained from the Changsheng Experimental Animal Centre of Liaoning Province, China (SCXK (Liao) 2020-0001), and housed in a specific pathogen-free experimental facility at Inner Mongolia University for Nationalities. The rats were kept under controlled conditions, with a temperature of 23±1°C, humidity of 55±5%, and a 12-hour light-dark cycle. They were given *ad libitum* access to food, water, and physical activity throughout the study period.

**2.3 Grouping of experimental animals and establishment of rat myocardial infarction model**

After one week of adaptive feeding, the rats were randomly assigned to a Control group, model group, and Agari-5 group. Rats in the model and Agari-5 groups underwent MI induction. Under isoflurane anesthesia, the animals were disinfected with alcohol, and a thoracotomy was performed to expose the heart. The pericardium was carefully torn to fully expose the heart, and the left anterior descending coronary artery (LADCA) was ligated with a No. 4-0 black silk thread to induce MI [10-12]. The specific experimental flow is shown in Figure 1.

#### 2.4 Experimental grouping and drug administration

In the control group and model group, an equivalent volume of saline was administered by gavage once daily. In the Agari-5 group, a dose of 0.8127 g/kg was given daily for six weeks at a fixed time. The gavage doses for all rats were adjusted based on the equivalent doses for animals and humans [13].

#### 2.5 Sample collection

Rats were anesthetized with isoflurane, and the abdominal cavity was opened to collect blood from the abdominal aorta. The blood was left at room temperature for 30 minutes and then centrifuged at 3500 rpm for 10 minutes. The supernatant was further centrifuged at 12,000 rpm for 10 minutes at 4°C and stored at -80°C. Heart tissue from the rats was also rapidly collected and stored at -80°C for further analysis.

#### 2.6 Creatine kinase, creatine kinase isoenzymes and lactate dehydrogenase activities in rats

The serum enzymatic activities of CK, CK-MB and LDH are key indicators used to assess myocardial injury. The procedure was carried out according to the manufacturer's instructions provided in the assay kits. Absorbance values for each well were measured at a wavelength of 450nm (optical density, OD).

#### 2.7 Hematoxylin and eosin staining and Masson's staining

After euthanizing the rats under anesthesia, tissue samples were collected and fixed in 10% neutral formaldehyde for 24 hours. The samples underwent gradient ethanol dehydration, xylene clearing, and paraffin embedding. Sections were then cut, stained with hematoxylin and eosin (HE) stain and Masson's stain, and sealed with neutral gum. The lesions were subsequently observed under a light microscope.

2.8 Proteomics sample preparation

Cardiac samples were collected and ground to a powder in liquid nitrogen. An appropriate amount of the powder was transferred to a 1.5 ml centrifuge tube and incubated with lysis buffer (8 M urea) containing 1 mM phenylmethylsulfonyl fluoride and 2 mM EDTA (final concentrations) for 5 minutes. The mixture was then sonicated on ice for 5 minutes (2 seconds on, 3 seconds off). The lysate was centrifuged at 4°C at 15000g for 20 minutes, and the supernatant was collected. The total protein concentration was determined using the bicinchoninic acid (BCA) protein quantification assay. An aliquot of the protein solution was taken based on the protein concentration and adjusted to a final volume of 200 µl with 8 M urea. The solution was reduced with 10 mM dithiothreitol for 45 minutes at 37°C and alkylated with 50 mM iodoacetamide for 15 minutes in the dark at room temperature. Pre-cooled acetone, four times the volume of the protein solution, was added to precipitate the proteins for 2 hours at -20°C. After centrifugation, the protein precipitate was air-dried and resuspended in 200 µl of 25 mM ammonium bicarbonate solution, followed by the addition of 3ul of trypsin (Promega) for overnight digestion at 37°C. After digestion, the peptides from each sample were desalted using a C18 column, concentrated by vacuum centrifugation, and redissolved in 0.1% (v/v) formic acid [14].

2.9 Liquid chromatography-tandem mass spectrometry detection

2.9.1 Nanoliter liquid chromatography detection

Samples were separated using a Vanquish Neo ultra-high-performance liquid chromatography (UHPLC) system[15]. The mobile phase consisted of phase A, which was a 0.1% formic acid aqueous solution, and phase B, which was a 0.1% formic acid acetonitrile solution (100% acetonitrile). The injection mode utilized a trap-analytical dual-column method, where the trap column was a PepMap Neo Trap Cartridge (300 µm x 5 mm, 5 µm) and the analytical column was an Easy-Spray™ PepMap™ Neo UHPLC column (150 µm x 15 cm, 2 µm). The temperature of the analytical column was maintained at 55°C using an integrated column oven. The sample volume was set at 200 ng, with a flow rate of 2.5 µl/min and an effective gradient duration of 6.9 minutes, resulting in a total run time of 8 minutes.

### 2.9.2 Orbitrap Astral mass spectrometer detection

Data-independent acquisition (DIA) analysis was carried out using a nanoscale Vanquish Neo system (Thermo Fisher Scientific) for chromatographic separation. Samples, following nanoscale HPLC separation, were analyzed by DIA mass spectrometry using an Orbitrap Astral high-resolution mass spectrometer (Thermo Scientific). The detection mode was set to positive ion, with a parent ion scanning range of 380-980 m/z and a primary mass spectral resolution of 240,000 at 200 m/z. The normalized automatic gain control (AGC) target was set at 500%, with a maximum ion injection time (IT) of 5 milliseconds. For MS<sup>2</sup> analysis, the DIA data acquisition mode was employed, utilizing 299 scanning windows. The isolation window was set to 2 Th, with an HCD collision energy of 25%. The normalized AGC Target was also 500%, and the maximum IT was set at 3 milliseconds.

### 2.10 Mass spectrometry data analysis

The library search software used for DIA mass spectrometry data in this study was DIA-NN (v1.8.1). The library was searched using the library-free method with the following search parameters: the database used was uniprot-proteome\_UP000002494\_Rat\_20220719.fasta database, which contained a total of 46,069 sequences, and the iRT2.fasta database, which included 1 sequence. The deep learning-based parameter was enabled to predict a spectral library. Additionally, the multiple bypass retrieval option was selected to generate a spectral library using DIA data, which was then utilized for reanalyzing the DIA data for protein quantification. Both precursor ions and protein-level false discovery rates were filtered at 1%, ensuring that the filtered data could be used for subsequent raw data analyses [16-17].

### 2.11 Bioinformatics analysis

To gain a comprehensive understanding of the functional properties of the identified and differentially expressed proteins, a thorough enrichment analysis was conducted. This analysis included the following components: Gene Ontology (GO) annotation, EuKaryotic Orthologous Groups (KOG) functional classification, Kyoto Encyclopedia of Genes and Genomes (KEGG) pathway analysis, protein domain characterization, subcellular localization assessment, and signal peptide prediction (using SignalP). The



differentially expressed proteins in each comparative group were enriched and analyzed at three levels: GO classification, KOG functional classification, and KEGG pathway analysis.

#### 2.12 Differently expressed protein interaction network

Protein-protein interaction (PPI) analysis was performed using the StringDB protein interaction database (<http://string-db.org/>). If a corresponding species was available in the database, the protein sequences of that species were directly extracted. If no corresponding species was found, protein sequences from a closely related species were utilized. The differentially expressed protein sequences were compared with the extracted sequences using BLAST, and interactions among the differentially expressed proteins were identified based on a confidence score greater than 400 (medium confidence). Static and dynamic network diagrams were constructed using R packages, specifically qgraph for static visualizations and networkD3 for dynamic visualizations.

#### 2.13 Western blot

Protein extraction was performed from the hearts of rats in each experimental group, and protein concentrations were quantified using a BCA kit. For protein analysis, 20 µg of each sample was loaded onto a 10% sodium dodecyl sulfate-polyacrylamide gel electrophoresis (SDS-PAGE) gel, where the proteins were separated according to their molecular weight during electrophoresis. After separation, the proteins were transferred from the gel to polyvinylidene fluoride (PVDF) membranes (Millipore, IPVH00010). To prevent nonspecific binding, the PVDF membranes were subjected to a 2-hour blocking process. Subsequently, the membranes were incubated overnight at 4°C with primary antibodies diluted 1:1000 to ensure optimal specificity and sensitivity. After the primary antibody incubation, the membranes were washed three times with phosphate-buffered saline (PBS) to remove any unbound antibodies. The membranes were then incubated with secondary antibodies diluted 1:5000 for 1 hour at room temperature, facilitating the detection of protein bands of interest. Finally, protein expression levels in the different experimental groups were compared [18].

#### 2.14 Statistical analysis

Statistical analysis was conducted using GraphPad Prism 8.0 (GraphPad Software). The



data are presented as mean±standard deviation (SD). Student's t-tests were used to evaluate differences between two groups, while one-way analysis of variance (ANOVA) was applied for multiple comparisons. Spearman's correlation analysis and the chi-square ( $\chi^2$ ) test were performed to assess correlations between different gene pairs. Survival differences were evaluated using the log-rank test. All statistical analyses were two-sided, with a significance level set at  $P<0.05$ , indicating statistical significance.

### 3. Results

#### 3.1 General condition of rats

The rats in the control group exhibited bright, lustrous fur, were highly responsive, and demonstrated normal eating and drinking behaviors, with no mortality occurring during the experimental period. In contrast, the rats in the model group displayed poor vitality, dull fur, cold skin, and a tendency to sleep excessively, along with considerably reduced food and water intake; some of these rats also had scanty stools. The rats in the Agari-5 group appeared to have slightly better vitality, though their fur lacked luster, and their complexion was somewhat warmer; however, they also exhibited slightly lower food and water intake compared to the control group. Body weight measurements revealed a steady increase in the control group each week, while the model group experienced a significant decrease in body weight. In contrast, the Agari-5 group showed an upward trend in body weight compared to the model group, indicating weight gain, as detailed in Supplementary Figure 1A.

#### 3.2 Cardiac function indicators

MI resulted in the destruction of cardiomyocytes, leading to increased activity levels of cardiac function enzymes, which are common indicators for detecting MI in rats. Compared to the control group, levels of CK, CK-MB and LDH were significantly elevated in the model group ( $P<0.05$ ), confirming the successful establishment of the model. In contrast, treatment with Agari-5 significantly reduced the cardiac function markers in rats with MI compared to the model group ( $P<0.05$ ). For further details, refer to Figures 1B-D.

#### 3.3 Hematoxylin and eosin staining and Masson's staining

As shown in Figures 2A-C, HE staining results indicated that the myocardial fibers in the control group were organized in bundles, with intact myocardial tissue structure and no evidence of inflammatory cell infiltration. Meanwhile, the model group exhibited disordered myocardial tissue, with blurred transverse striations and a significant enlargement of the myocardial interstitial space, accompanied by extensive inflammatory cell infiltration. Compared to the model group, the myocardial fibers in the Agari-5 group were more organized, showing improved cytoplasmic edema and more intact cytoplasmic nuclei. As illustrated in Figure 3A-C, Masson staining revealed no significant collagen fiber deposition in the myocardial tissue of the control group. In the model group, normal myocardial fibers were damaged, with extensive collagen fiber deposits observed, indicating pronounced myocardial fibrosis and atrophic degeneration, along with inflammatory cell infiltration in the infarcted areas. In the Agari-5 group, myocardial fibrosis was significantly reduced, with fewer collagen fibers deposited and diminished inflammatory cell infiltration.

3.4 Quality assessment of quantitative proteomics results

In constructing the mathematical model, principal component analysis (PCA) was initially employed to process the overall data, allowing for the observation of the natural distribution of experimental samples and group relationships. The distribution of each group, as shown in Figures 1B-C of the Annex, was classified satisfactorily, indicating clear differences in protein expression among the groups. Correlation analysis between samples within each group is presented in Annex Figure 1D. This analysis enables the observation of biological replicates among samples within the same group. The results demonstrate that the correlation coefficients of samples within each group are higher than those of samples between groups, suggesting that the differential proteins identified in this experiment are more reliable.

3.5 Differential protein expression

In the analysis of differential protein expression, a total of 231 proteins were identified in the control group compared with the model group, with 122 proteins being up-regulated and 109 down-regulated, as shown in Figure 4A. In the comparison between the Agari-5 group and the model group, 190 proteins were identified, of which 99 were

up-regulated and 91 were down-regulated, as displayed in Figure 4B. Finally, Figure 4C shows that in the Agari-5 group compared to the control group, 246 proteins were identified, with 129 proteins up-regulated and 117 down-regulated.

### 3.6 Bioinformatics analysis

#### 3.6.1 Functional annotation of differentially expressed proteins

GO is an international standard classification system for gene functions, comprising three main components: Biological Process, Molecular Function, and Cellular Component. The differentially expressed proteins annotated to secondary GO entries were counted, and each classification displayed the top 20 GO terms with the highest-ranked differentially expressed proteins (in descending order). The results are presented in Figure 2A-C in the Appendix. In the Biological Process category, the groups include cellular process, metabolic process, biological regulation, and cellular component. Molecular Function is primarily characterized by cellular anatomical entity and protein-containing complexes. Cellular Component is mainly represented by binding activities. This study was annotated using the KOG database, and the number of differentially expressed proteins within each KOG category was counted and displayed in a bar chart (Figure 2D-F in the Appendix). The categories included posttranslational modification, protein turnover, chaperones, general function prediction only, signal transduction mechanisms, and others, highlighting the functional groups of proteins identified in each experimental comparison.

KEGG pathways mainly encompass areas such as metabolism, genetic information processing, environmental information processing, cellular processes, human diseases, and drug development. Pathway analysis allows for the identification of critical biochemical metabolic and signal transduction pathways in which the differentially expressed proteins are involved. Annex Figure 2G-I presents the top KEGG pathways identified, which include biosynthesis of amino acids, carbon metabolism, purine metabolism, thermogenesis, and Th17 cell differentiation.

#### 3.6.2 Functional enrichment of differentially expressed proteins

In the enrichment analysis, the 50 GO terms with the highest P-values (in descending order) were selected and visualized in bar charts, as shown in Figure 5A-C. For

Biological Process, the dominant terms included signal transduction, negative regulation of transcription by RNA polymerase II, and innate immune response. In Molecular Function, the prominent categories were metal ion binding, adenosine triphosphate (ATP) binding, and protein homodimerization activity. In Cellular Component, key categories included extracellular space, integral component of the membrane, and Golgi apparatus. From the KOG enrichment analysis, 20 functional categories with the top P-value rankings (sorted from smallest to largest) were selected and visualized using bubble diagrams (Figure 5D-F). The dominant pathways included general function prediction only, signal transduction mechanisms, amino acid transport and metabolism, and carbohydrate transport and metabolism. For the KEGG enrichment analysis results (Figure 5G-I), bubble diagrams were used to represent the degree of enrichment based on fold enrichment, P-value, and the number of differentially expressed proteins involved. Key enriched pathways included biosynthesis of amino acids, cell adhesion molecules, drug metabolism, Th17 cell differentiation, and biosynthesis of cofactors.

3.6.3 Interaction network analysis of differentially expressed proteins

The results of the PPI interaction network analysis are displayed in Figures 6A-C. These networks can be imported into Cytoscape software for further visual editing and exploration. In the comparison between the control group and model group, 144 nodes were identified. In the Agari-5 group versus the model group, 112 nodes were found. Between the Agari-5 group and the control group, 168 nodes were identified. In total, the analysis revealed 60 differential proteins, detailed in Table 1.

3.7 Immunoblot analysis of differentially expressed proteins in rat heart tissue

The levels of differentially expressed proteins in rat heart tissues were evaluated through Western blot analysis. Based on the proteomics data, four key proteins were identified: SDF2, PDK1, SMAD4, and PSAT1. For SDF2, PDK1, and SMAD4, protein expression levels in the model group were found to be decreased compared to the control group, though the differences were not statistically significant ( $P>0.05$ ). In contrast, the Agari-5 group showed an up-regulation trend in the expression levels of these proteins compared to the model group, though again, without statistical

significance ( $P>0.05$ ). Regarding PSAT1, its expression in the model group was up-regulated relative to the control group ( $P>0.05$ ). However, the Agari-5 group exhibited a trend of down-regulated PSAT1 expression compared to the model group, though this change was not statistically significant ( $P>0.05$ ). The protein bands are shown in Figure 7A, and the corresponding statistical bar graphs are displayed in Figures 7B-E.

#### 4. Discussion

In recent decades, natural medicines have gained significant use in clinical treatment for various diseases[19-22]. Cardiovascular disease remains a leading cause of mortality and morbidity worldwide. Studies have demonstrated that traditional Mongolian medicine preparations, such as Sanwei Tanxiang Decoction, can alleviate acute ischemia-reperfusion injury by modulating the electrophysiological properties of rat cardiomyocytes[23]. Similarly, the extract from Sugmul-3, another Mongolian medicine, has shown protective effects against isoproterenol-induced heart failure in Wistar rats by regulating mitochondrial dynamics[24]. Mongolian medicine emphasizes a holistic view of the human body, treating diseases through the interaction of multiple drugs. This approach offers advantages such as fewer adverse reactions and side effects, particularly in preventing and treating cardiovascular diseases. Agari-5 is a widely used traditional compound in Mongolian medicine for managing cardiovascular diseases[25]. Its multi-component and multi-target characteristics enhance its effectiveness in treating cardiovascular diseases[26]. Among the key components of Agari-5 is *Salvia miltiorrhiza*, which plays a critical role in reducing myocardial fibrosis, delaying cardiac remodeling[27], reducing myocardial inflammation and injury[28,29], and decreasing oxidative stress and injury[30,31]. Therefore, understanding the protective mechanisms of Agari-5 is essential for guiding clinical use, improving patient outcomes, and enhancing the prognosis, treatment, and overall quality of life for individuals with cardiovascular diseases.

In this study, an MI rat model was established to assess cardiac function indices and the pathological changes in cardiac tissues. The results demonstrated that, compared to the control group, the cardiac function indices in the model group were significantly

elevated, while pathological findings showed disorganized myocardial tissue structure, with blurred transverse striations, markedly enlarged myocardial gaps, and extensive infiltration by inflammatory cells. However, following treatment with Agari-5, both cardiac function and myocardial tissue pathology improved. Notably, the degree of myocardial fibrosis was markedly reduced, with less collagen fiber deposition and decreased inflammatory cell infiltration. These findings suggest that the therapeutic effect of the Agari-5 compound may be attributed to the interactions of its components. In the proteomics study, the results showed a clear distribution and high dispersion between groups, indicating reliable findings for differential protein expression. Comparisons between the groups revealed a range of 190 to 246 differentially expressed proteins, while enrichment analyses suggested that the therapeutic mechanism of Agari-5 in rats following MI may involve alterations in processes such as fatty acid degradation, metabolism, elongation, carbon metabolism, and protein digestion and absorption, all of which are vital for energy metabolism. Furthermore, differential protein function annotation analysis identified cardiovascular-related proteins in biological processes. These findings also indicated that Agari-5 may act on pathways related to myocardial fibrosis and mitochondrial energy metabolism in cardiomyocytes after MI. Together, the differential protein annotations and enrichment analyses suggest that Agari-5 may exert a therapeutic effect on MI by modulating these pathways.

In the PPI analysis, a total of 60 proteins were identified, with four specific proteins (SDF2, PDK1, SMAD4, PSAT1) receiving attention due to their potential role as biomarkers for MI diagnosis. The SMAD4 signaling pathway has been reported to have a close association with cardiovascular disease, where its activation can lead to myocardial injury [32] and is significantly involved in the progression of myocardial fibrosis [33]. PDK1 plays a key role in cellular phosphorylation processes related to mitochondrial energy metabolism, such as maintaining mitochondrial membrane potential, ATP generation, and calcium uptake[34]. In this study, we used Western blotting to investigate the expression levels of these differential proteins. These results showed that, in MI rats treated with Agari-5, the expression levels of these proteins was

comparable to those in the control group, suggesting that SDF2, PDK1, SMAD4, and PSAT1 may be important targets influenced by Agari-5. This study applied a logical approach of “disease-drug-target” to preliminarily verify the efficacy of Agari-5 in treating MI in rats. Moreover, through proteomic analysis, the research delved deeper into the protective mechanisms of Mongolian traditional medicine formulas, finding that these traditional formulas may protect MI rats through the regulation of multiple protein targets and molecular mechanisms, such as multi-component interactions and synergistic effects, providing a new direction for research on national medicines and offering a reference for clinical treatments of cardiovascular diseases.

## 5. Conclusion

In conclusion, this study successfully identified the potential therapeutic benefits and mechanisms by which Agari-5 exerts its effects against MI. The findings provide initial evidence supporting the use of Agari-5 as a treatment for cardiovascular diseases and cardiac injuries, highlighting its possible role as an effective strategy in clinical settings.

### Data availability statement

The study's original contributions are contained in the publication or supplemental material; the corresponding author can be contacted with any additional questions.

### Ethics statement

The studies involving animals were approved by the local Ethics Committee of Affiliated Hospital of Inner Mongolia Minzu University(No.NM-LL-2024-05-16-08). Strictly in accordance with the requirements of the Animal Ethics Committee.

### Author contributions

YZ: Formal analysis, Writing-original draft. HQ: Data curation and Formal analysis. ZB and YT: Validation and Methodology. XQ, YB and MS: Formal analysis and Data curation. QW: Investigation, Methodology and Writing-review & editing.



Funding

This study was supported by the Xinganmeng Science and Technology Programme Project(MBJH2023022).

Conflict of interest

The study was carried out without any financial or commercial ties that can be seen as a possible conflict of interest, according to the authors.

References

[1] Nowbar NA, Gitto Mauro, Howard JP, Francis DP, Al-Lamee Rasha, Mortality From Ischemic Heart Disease. *Circ Cardiovasc Qual Outcomes*. 2019 Jun;12:e005375. doi: 10.1161/CIRCOUTCOMES.118.005375.

[2] Kassebaum NJ, Arora M, Barber RM, Bhutta ZA, Brown J, Carter A, et al. Global, regional, and national disability-adjusted life-years (DALYs) for 315 diseases and injuries and healthy life expectancy (HALE), 1990–2015: a systematic analysis for the Global Burden of Disease Study 2015. *Lancet*. 2016 Oct; 388:1603-1658. doi: 10.1016/S0140-6736(16)31460-X.

[3] Davis BH, Morimoto Y, Sample C, Olbrich K, Leddy HA, Guilak F, Taylor DA. Effects of myocardial infarction on the distribution and transport of nutrients and oxygen in porcine myocardium. *J Biomech Eng*. 2012 Oct;134:101005. doi: 10.1115/1.4007455.

[4] Jimenez RF, Vivas D, García-Rubira GC, Fernandez-Ortiz A, Balbacid E, Kallmeyer A, et al. Profound myocardial ischemia associated to occlusion of the right coronary artery. *Int J Cardiol*. 2011 Jun; 149:e123-4. doi: 10.1016/j.ijcard.2009.06.017.

[5] Frangogiannis NG. Pathophysiology of myocardial infarction. *Compr Physiol*. 2015 Sep; 5:1841-75. doi: 10.1002/cphy.c150006.

[6] Wang J, Li L, Ma N, Zhang XH, Qiao YY, Fang GJ, et al. Clinical investigation of acute myocardial infarction according to age subsets. *Exp Ther Med*. 2020 Nov; 20:120. doi: 10.3892/etm.2020.9248.

- [7] Hernandez AF, Udell JA, Jones WS, Anker SD, Petrie MC, Harrington J, et al. Effect of Empagliflozin on Heart Failure Outcomes After Acute Myocardial Infarction: Insights From the EMPACT-MI Trial. *Circulation*. 2024 May;149:1627-1638. doi: 10.1161/CIRCULATIONAHA.124.069217.
- [8] Wasinger VC, Cordwell SJ, Poljak AC, Yan JX, Gooley AA, Wilkins MR, et al. Progress with gene-product mapping of the Mollicutes: *Mycoplasma genitalium*. *Electrophoresis*. 1995 Jul;16:1090-4. doi: 10.1002/elps.11501601185.
- [9] Yang H, Song ML, Lan SW, Ying X. Overview of Mongolian Medicine for Coronary Heart Disease. *J Inner Mongolia Minzu University(Natural Sciences Edition)*, 2020; 35:437-443.
- [10] Hou Y, Huang C, Cai X, Zhao J, Guo W. Improvements in the establishment of a rat myocardial infarction model. *J Int Med Res*. 2011;39:1284-92. doi: 10.1177/147323001103900416.
- [11] Zhang HY, Chen X, Hu P, Liang QL, Liang XP, Wang YM, et al. Metabolomic profiling of rat serum associated with isoproterenol-induced myocardial infarction using ultra-performance liquid chromatography/time-of-flight mass spectrometry and multivariate analysis. *Talanta*. 2009 Jul;79:254-9. doi: 10.1016/j.talanta.2009.03.045.
- [12] Wang JW, Liu XL, Ren B, Rupp H, Takeda N, Dhalla NS. Modification of myosin gene expression by imidapril in failing heart due to myocardial infarction. *J Mol Cell Cardiol*. 2002 Jul;34:847-57. doi: 10.1006/jmcc.2002.2023.
- [13] Han HJ, Hui HX, Yang CZ, Shan ZQ, Yuan SR. Does conversion among different animals and healthy volunteers in pharmacological study. *Chinese Journal of Clinical Pharmacology and Therapeutics*. 2004;1069-1072.
- [14] Ross PL, Huang YN, Marchese JN, Williamson B, Parker K, Hattan S, et al. Multiplexed protein quantitation in *Saccharomyces cerevisiae* using amine-reactive isobaric tagging reagents. *Mol Cell Proteomics*. 2004 Dec;3:1154-69. doi: 10.1074/mcp.M400129-MCP200.
- [15] Wu J, Xie XL, Liu YS, He JT, Benitez R, Buckanovich RJ, et al. Identification and Confirmation of Differentially Expressed Fucosylated Glycoproteins in the Serum of Ovarian Cancer Patients Using a Lectin Array and Lc-Ms/Ms. *J Proteome Res*. 2012

Seep; 11:4541-52. doi: 10.1021/pr300330z.

[16] Prianchnikov N, Koch H, Koch S, Lubeck M, Heilig R, Brehmer S, et al. MaxQuant Software for Ion Mobility Enhanced Shotgun Proteomics. *Mol Cell Proteomics*. 2020 Jun;19:1058-1069. doi: 10.1074/mcp.TIR119.001720.

[17] Yu FC, Haynes SE, Teo GC, Avtonomov DM, Polasky DA, Nesvizhskii AI. Fast Quantitative Analysis of timsTOF PASEF Data with MSFRAGGER and IONQUANT. *Mol Cell Proteomics*. 2020 Sep;19:1575-1585. doi: 10.1074/mcp.TIR120.002048.

[18] Xu DJ, Liu LB, Zhao YJ, Yang L, Cheng JY, Hua RM, et al. Melatonin protects mouse testes from palmitic acid-induced lipotoxicity by attenuating oxidative stress and DNA damage in a SIRT1-dependent manner. *J Pineal Res*. 2020 Nov; 69:e12690. doi: 10.1111/jpi.12690.

[19] Li TT, Wang ZB, Li Y, Cao F, Yang BY, Kuang HX. The mechanisms of traditional Chinese medicine underlying the prevention and treatment of atherosclerosis. *Chin J Nat Med*. 2019 Jun;17:401-412. doi: 10.1016/S1875-5364(19)30048-2.

[20] Hao P P, Jiang F, Chen YG, Yang JM, Zhang K, Zhang MX, et al. Traditional Chinese medication for cardiovascular disease. *Nat Rev Cardiol*. 2015 Jun;12:318. doi: 10.1038/nrcardio.2015.60.

[21] Xiong NN, Zou YQ, Huang XW, Gong LJ, Yu CH, Zou YX. Effects of TCM therapy on the progression of chronic renal failure caused by primary glomerulonephritis. *J Tradit Chin Med*. 1988 Jun;8(2):107-11.

[22] Lee W, Ku SK, Min BW, Lee S, Jee JG, Kim JA, et al. Vascular barrier protective effects of pellitorine in LPS-induced inflammation in vitro and in vivo. *Fitoterapia*. 2014 Jan;92:177-87. doi: 10.1016/j.fitote.2013.11.006.

[23] Wan Q, Wang Y, Yong M, Hu PF, Liang CG, Yang XJ, et al. Sanwei sandalwood decoction ameliorates acute ischemia-reperfusion injury in rats by modulating myocyte electrophysiological characteristics. *Biomed Pharmacother*. 2023 Feb;158:114103. doi: 10.1016/j.biopha.2022.114103.

[24] Zhen D, Na RS, Wang Y, Bai X, Fu DN, Wei CX, et al. Cardioprotective effect of ethanol extracts of Sugemule-3 decoction on isoproterenol-induced heart failure in Wistar rats through regulation of mitochondrial dynamics. *J Ethnopharmacol*. 2022 Jun;

28:292:114669. doi: 10.1016/j.jep.2021.114669.

[25] Zhang X, Ren FY. Determination of tanshinone IIA in Ulan Agar-5 by high performance liquid chromatography. *Chinese Journal of Hospital Pharmacy*, 2008; 317-318.

[26] Zhang SD, Shan L, Li Q, Wang X, Li SL, Zhang Y, et al. Systematic Analysis of the Multiple Bioactivities of Green Tea through a Network Pharmacology Approach. *Evid Based Complement Alternat Med*. 2014;512081. doi: 10.1155/2014/512081.

[27] Liu T, Song DL, Dong JZ, Zhu PH, Liu J, Liu W, et al. Current understanding of the pathophysiology of myocardial fibrosis and its quantitative assessment in heart failure. *Front Physiol*. 2017 Apr;24:8:238. doi: 10.3389/fphys.2017.00238.

[28] Dutka M, Bobiński R, Ulman-Włodarz I, Hajduga M, Bujok J, Pająk C, et al. Various aspects of inflammation in heart failure. *Heart Fail Rev*. 2020 May; 25:537-548. doi: 10.1007/s10741-019-09875-1.

[29] Dawuti A, Sun SC, Wang RR, Gong DF, Liu RQ, Kong DW, et al. Salvianolic acid A alleviates heart failure with preserved ejection fraction via regulating TLR/Myd88/TRAF/NF- $\kappa$ B and p38MAPK/CREB signaling pathways. *Biomed Pharmacother*. 2023 Dec;168:115837. doi: 10.1016/j.biopha.2023.115837.

[30] Pol A, Gilst WH, Voors AA, Meer P. Treating oxidative stress in heart failure: past, present and future. *Eur J Heart Fail*. 2019 Apr;21:425-435. doi: 10.1002/ejhf.1320.

[31] Chen RJ, Chen WL, Huang XL, Rui QL. Tanshinone IIA attenuates heart failure via inhibiting . *Mol Med Rep*. 2021 Jun;23:404. doi: 10.3892/mmr.2021.12043.

[32] Xue D, Sun JL, Yang J. Early L-T4 intervention improves fetal heart development in pregnant rats with subclinical hypothyroidism rats by activating BMP4/Smad4 signaling pathway. *BMC Cardiovasc Disord*. 2020 Aug;20:369. doi: 10.1186/s12872-020-01646-3.

[33] Sun RR. The influence of huangqibaoxin decoction and the effective components salvianolic acid B on myocardial fibrosis and TGF -  $\beta$ / smad signal of rats with dilated cardiomyopathy. *Nanjing University of Chinese Medicine*, 2017.

[34] Betz C, Stracka D, Prescianotto-Baschong C, Frieden M, Demarex N, Hall

1  
2  
3  
4  
5  
6  
7  
8  
9  
10  
11  
12  
13  
14  
15  
16  
17  
18  
19  
20  
21  
22  
23  
24  
25  
26  
27  
28  
29  
30  
31  
32  
33  
34  
35  
36  
37  
38  
39  
40  
41  
42  
43  
44  
45  
46  
47  
48  
49  
50  
51  
52  
53  
54  
55  
56  
57  
58  
59  
60

MN.Feature Article: m TOR complex 2-Akt signaling at mitochondria-associated endoplasmic reticulum membranes (MAM) regulates mitochondrial physiology. Proc Natl Acad Sci USA. 2013 Jul;110:12526-34. doi: 10.1073/pnas.1302455110.

For Peer Review

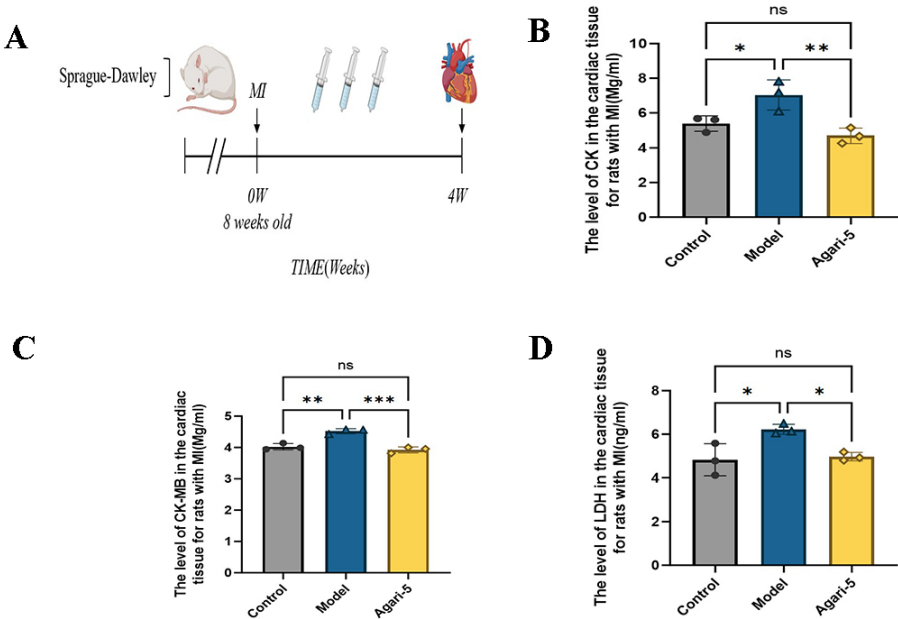


**Fig. 1: A: Flow chart of animal experiment; B-E: Histogram of cardiac function indexes in rats (n=3,mean±SD).**

Fig. 1: A: Flow chart of animal experiment; B-E: Histogram of cardiac function indexes in rats (n=3, mean±SD).

93x86mm (300 x 300 DPI)



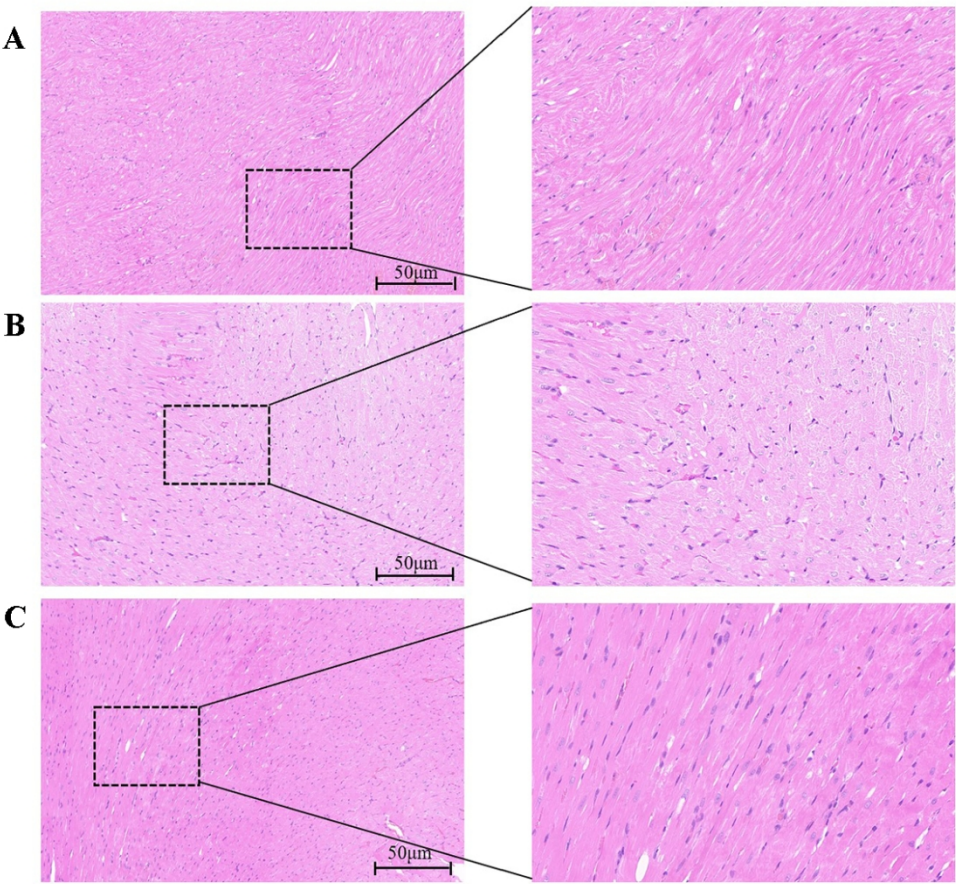


**Fig. 2** HE staining results of rats in each group(A is the Control group, B is the Model group and C is the Agari-5 group)

HE staining results of rats in each group (A is the control group, B is the model group, and C is the Agari-5 group)

99x102mm (300 x 300 DPI)



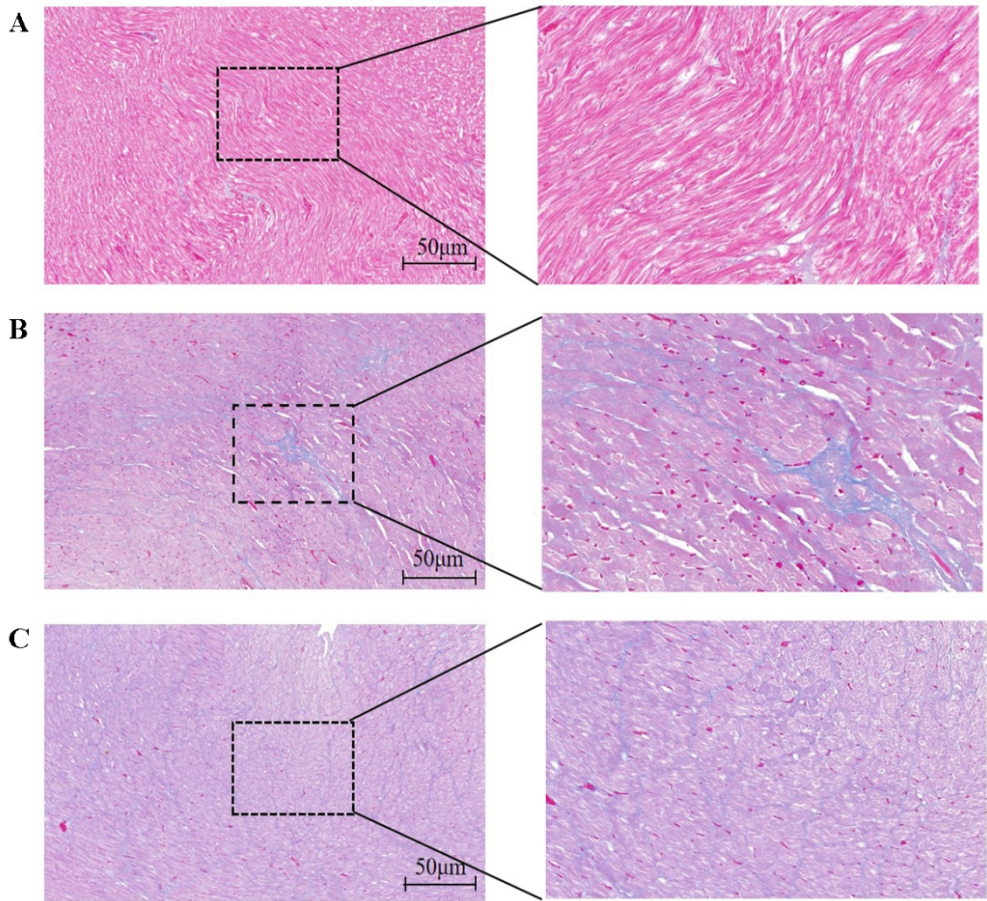


**Figure 3:Masson staining results of rats in each groups (A is the Control group;B is the Model group;C is the Agari-5 goup)**

Masson staining results of rats in each group (A is the control group, B is the model group, and C is the Agari-5 group)

99x103mm (300 x 300 DPI)

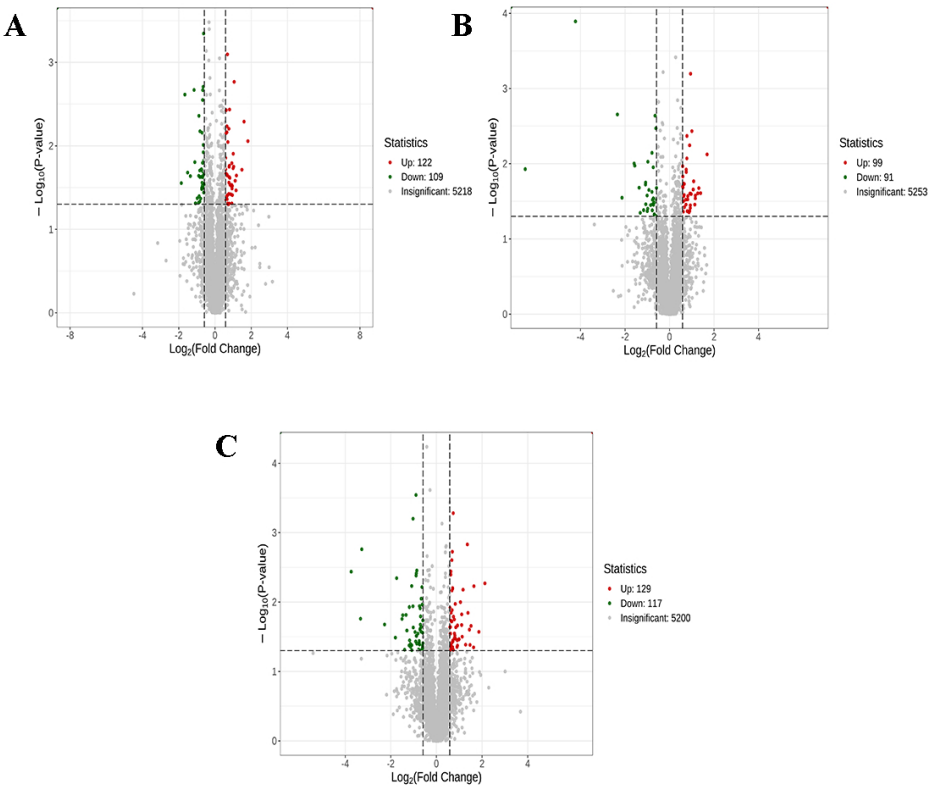


**Fig. 4** Volcano plot of differential proteins between groups of rats, note: horizontal coordinates represent differential fold's taken logarithmically at the base of 2, vertical coordinates represent P-values taken logarithmically at the base of 10, and red and green scatters represent up- and down-regulated differential proteins, respectively.

Volcano plot of differential proteins between groups of rats. Note: horizontal coordinates represent differential folds taken logarithmically at the base of 2, vertical coordinates represent P-values taken logarithmically at the base of 10, and red and green scatters represent up- and down-regulated differential proteins, respectively.

99x98mm (300 x 300 DPI)

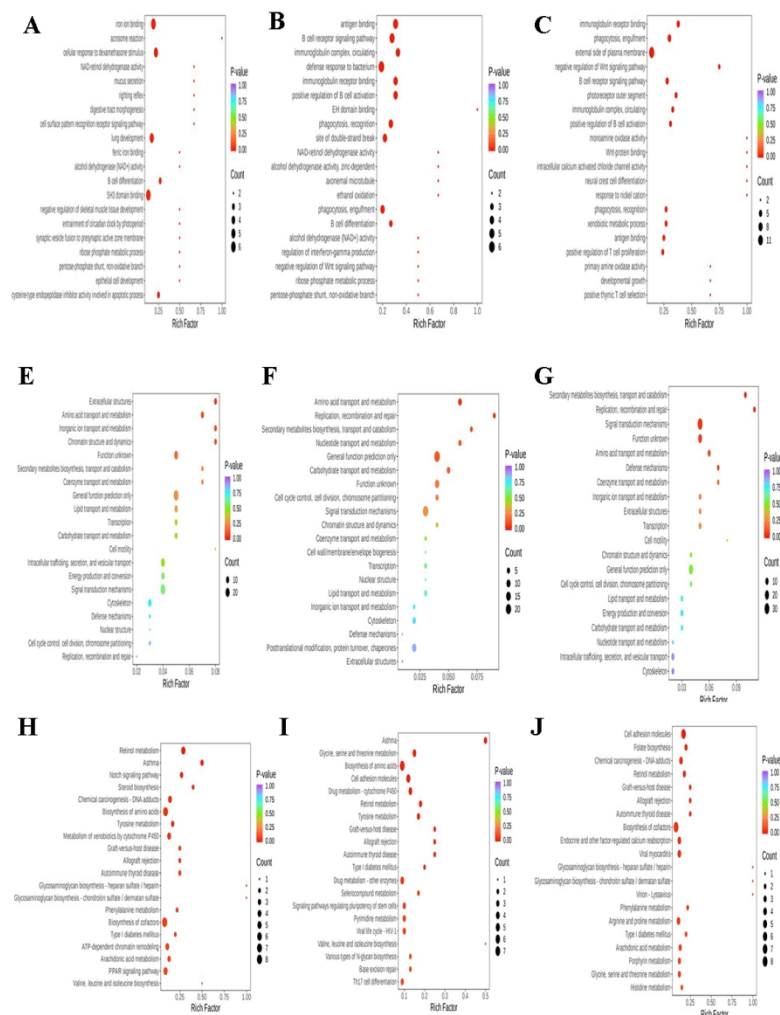


**Fig. 5** Bubble diagram of enrichment analysis of differentially expressed proteins GO, KOG, KEGG. Note: The horizontal coordinate represents the enrichment multiplicity (the ratio of the number of differentially expressed proteins enriched to the number of proteins annotated in the entry), the higher enrichment multiplicity indicates the higher degree of enrichment of differentially expressed proteins, and the vertical coordinate represents the name of the entries of GO, KOG, and KEGG.

Bubble diagram of enrichment analysis of differentially expressed proteins GO, KOG, KEGG. Note: The horizontal coordinate represents the enrichment multiplicity (the ratio of the number of differentially expressed proteins enriched to the number of proteins annotated in the entry), the higher enrichment multiplicity indicates the higher degree of enrichment of differentially expressed proteins, and the vertical coordinate represents the name of the entries of GO, KOG, and KEGG.

99x152mm (300 x 300 DPI)

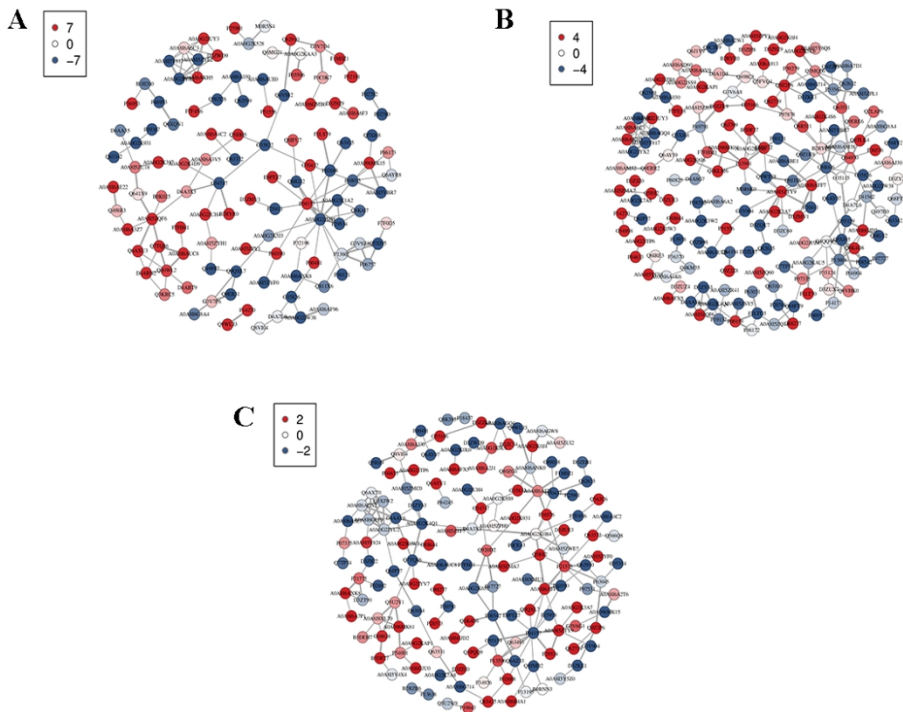


**Fig. 6 Interaction network diagram of differentially expressed proteins among groups, Note:Each node in the interaction network represents a differentially expressed protein, node red (up) represents that the expression level of differentially expressed proteins is up-regulated, node blue (down) represents that the expression level of differentially expressed proteins is down-regulated(A is the Control group, B is the Model group and C is the Agari-5 group).**

Interaction network diagram of differentially expressed proteins among groups, Note:Each node in the interaction network represents a differentially expressed protein, node red (up) represents that the expression level of differentially expressed proteins is up-regulated, node blue (down) represents that the expression level of differentially expressed proteins is down-regulated(A is the Control group;B is the Model group;C is the Agari-5 group).

99x99mm (300 x 300 DPI)

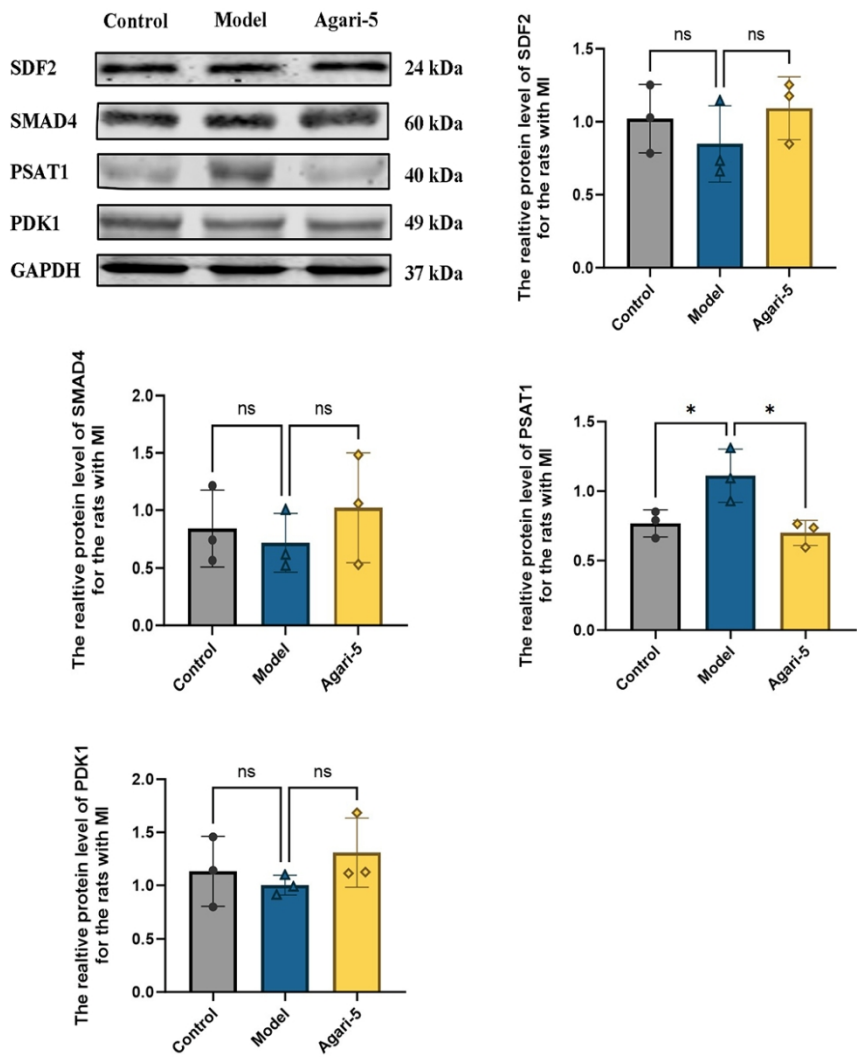


Fig. 7 A is the protein bar graph and B-E are the statistical histograms of each protein (n=3,mean±SD).

A is the protein bar graph and B-E are the statistical histograms of each protein (n=3,mean±SD).

99x119mm (300 x 300 DPI)

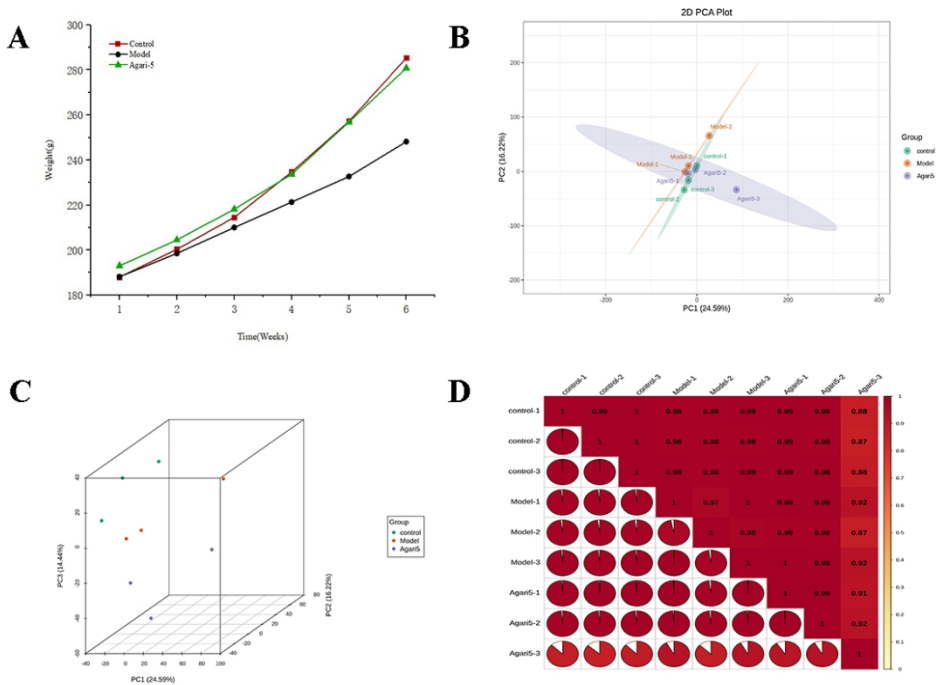
Table 1 Statistical Table of Differential Protein Expression

Gene	Agari5 vs Model Regulation	Model vs control Regulation	Agari5 vs control Regulation
Neb	up	down	insig
Pnkp	up	down	insig
Papss1	up	down	insig
Lonrf1	up	down	insig
Psat1	down	up	insig
Ccser2	up	down	insig
Man1c1	down	up	insig
Smoc1	down	up	insig
AC095947.1	up	down	insig
Nxn	up	down	insig
Tanc1	up	down	insig
Sdf2	up	down	insig
Syap1	up	down	insig
Dmc1	up	down	insig
Nom1	up	down	insig
Decr1	down	up	insig
Rnpep	down	up	insig
Pdk1	up	down	insig
Isg15	up	down	insig
Trio	up	down	insig
Trim32	up	down	insig
Csnk2a2	up	down	insig
Chgb	up	down	insig
Cdk18	down	up	insig
Pold1	down	up	insig
Smad4	up	down	insig
Otc	up	down	insig
Mbp	down	up	insig
Psbpc1	down	up	insig
Ptpcr	up	down	insig
Grb10	up	down	insig
Pth1r	up	down	insig
Slc6a7	down	up	insig
Vcam1	down	up	insig
Map1a	down	up	insig
Afm	up	down	insig
Il6st	up	down	insig
Padi3	up	down	insig
Ermard	down	up	insig
Gramd1a	up	down	Insig



Znf830	down	up	insig
Lztf11	down	up	insig
Cep70	down	up	insig
Armex3	up	down	insig
Synj1	up	down	insig
Nrxn1	down	up	insig
Prx	down	up	insig
Ces1f	down	up	insig
Isg20l2	up	down	insig
Dync2li1	down	up	insig
Blvra	up	down	insig
Krt42	up	down	insig
Tepp	down	up	insig
Fmo2	up	down	insig
Wls	up	down	insig
Rsl1d1l1	up	down	insig
Asrgl1	down	up	insig
Ttl	up	down	insig
Nme7	down	up	insig
Pde4dip	up	down	insig

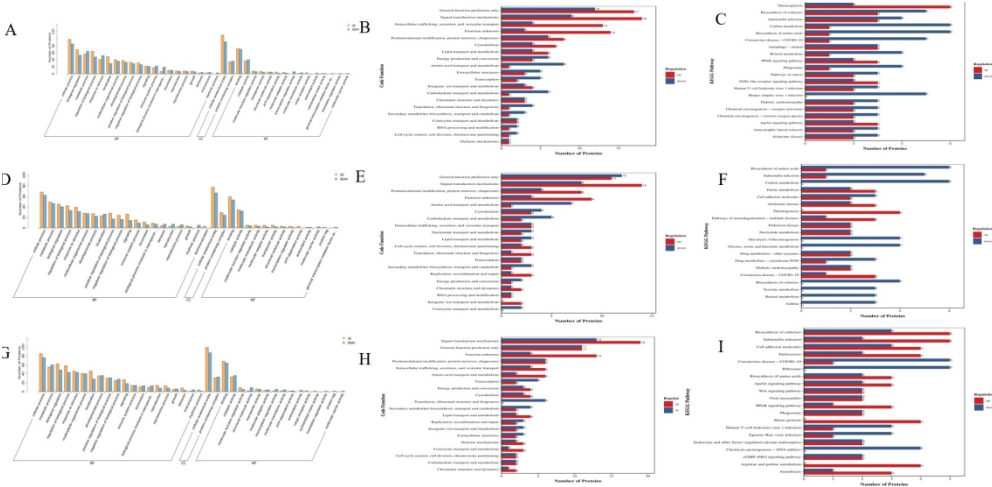




**Supplementary Figure 1:**A: Changes in body weight of rats in each group; B-C: Results of 2D and 3D PCA analysis; D: Inter-sample correlation plots, Note: Horizontal and vertical coordinates represent the names of the samples, and the change of colour from red to yellow represents the change of correlation from high to low. The size of the fan area in the graph represents the size of the correlation coefficient of the corresponding samples in horizontal and vertical coordinates; the numbers in the graph represent the correlation coefficients of the corresponding samples in horizontal and vertical coordinates.

Changes in body weight of rats in each group; B-C: Results of 2D and 3D PCA analysis; D: Inter-sample correlation plots, Note: Horizontal and vertical coordinates represent the names of the samples, and the change of color from red to yellow represents the change of correlation from high to low. The size of the fan area in the graph represents the size of the correlation coefficient of the corresponding samples in horizontal and vertical coordinates; the numbers in the graph represent the correlation coefficients of the corresponding samples in horizontal and vertical coordinates.

99x114mm (300 x 300 DPI)



Supplementary Figure 2: A-C: Up- and down-regulated differentially expressed proteins GO classification histograms. D-F: Comparison of up- and down-regulated differentially expressed proteins KOG annotations bar chart. G-I: Comparison of the up- and down-regulated differentially expressed proteins of the KEGG classifications bar chart.(A,D,G is Agari-5 vs Control; B,E,H is Agari-5 vs Model; C,F,I is Model vs Control)

A-C: Up-and down-regulated differentially expressed proteins GO classification histograms. D-F: Comparison of up- and down-regulated differentially expressed proteins KOG annotations bar chart. G-I: Comparison of the up- and down-regulated differentially expressed proteins of the KEGG classifications bar chart. (A, D, and G are Agari-5 vs. Control; B, E, and H are Agari-5 vs. Model; C, F, and I are Model vs. Control.)

274x150mm (192 x 192 DPI)